

Z POLARIZATION IN $pp \rightarrow ZZ \rightarrow \ell^+\ell^-\nu\bar{\nu}$ AT THE LHC

M. J. DUNCAN and M. H. RENO*

*Department of Physics and Astronomy, University of Iowa, Iowa City,
Iowa 52242, USA*

ABSTRACT

We evaluate the feasibility of measuring the Z polarization from a heavy Higgs signal in the decay channel $H \rightarrow ZZ \rightarrow \ell^+\ell^-\nu\bar{\nu}$. Including gluon fusion production of the Higgs, continuum production of Z pairs and the QCD background of single Z production with a missing jet, we find that the average value of a new variable to measure the Z polarization, as a function of transverse mass, will demonstrate the existence of a Higgs boson for heavy Higgs masses up to 800 GeV at the LHC with an integrated luminosity of 10^5 pb $^{-1}$.

1. Introduction

The ‘gold-plated’ heavy Higgs decay mode $H \rightarrow ZZ \rightarrow \ell_1^+\ell_1^-\ell_2^+\ell_2^-$ has received much attention in the literature because of the opportunity for a fully reconstructed Higgs signal.¹ For Higgs masses near the unitarity limit of 800 GeV,² however, the event rates are low for pp production of the Higgs boson at the Large Hadron Collider (LHC) center of mass energy $\sqrt{S} = 14$ TeV. To augment the Higgs search in the high mass region, the Higgs decay mode $H \rightarrow ZZ \rightarrow \ell^+\ell^-\nu\bar{\nu}$ should also be considered as it is enhanced relative to the gold-plated decay mode by a factor of six.³ This mode is easily identifiable by the large missing transverse momentum in the event and a pair of charged leptons that reconstruct to the Z mass. In addition to searching for an enhancement in the event rate, best identified in the transverse mass distribution,⁴ one can also use polarization information to identify a Higgs signal. The Higgs boson decays preferentially into longitudinally polarized Z ’s, (Z_L) while the irreducible and reducible backgrounds to $pp \rightarrow \ell^+\ell^- + \text{missing } p_T$ involve primarily transversely polarized Z ’s (Z_T). Polarization methods have been adopted for the gold-plated mode⁵ and the WW final state⁶, and we have suggested that this be applied to the case of $pp \rightarrow ZZ \rightarrow \ell^+\ell^-\nu\bar{\nu}$.⁷ Here, we demonstrate that even with the QCD background included, the LHC with an integrated luminosity of $\mathcal{L} = 10^5$ pb $^{-1}$ has a capability of distinguishing Higgs boson production in the $\ell^+\ell^-\nu\bar{\nu}$ decay mode from the background signal for a range of heavy Higgs masses m_H up to 800 GeV. We consider here masses between 400 GeV and 800 GeV.

*Presenter. Work supported in part by National Science Foundation Grant No. PHY-9307213.

2. Signal and Backgrounds

The Higgs coupling to other particles is proportional to the particle's mass, so the main contributions to Higgs production involve top quarks and weak gauge bosons. Gunion *et al.*⁸ have shown that production of the Higgs, with $t\bar{t}$ in the final state is very small. The main Higgs production processes are gluon fusion into a top quark loop, which couples to the Higgs, and vector boson fusion into a Higgs. For a top quark mass of 175 GeV, the gluon fusion mechanism dominates vector boson fusion for the full range of Higgs masses of interest: $m_H = 400 - 800$ GeV. The vector boson fusion cross section $qq \rightarrow qqZZ$ with an s -channel Higgs, for Higgs masses between 400 GeV and 800 GeV, lies below the gluon fusion cross section by a factor of ~ 10 at the low mass end, to a factor of ~ 3 at the high mass end. Baur and Glover⁹ have done the full calculation of $ZZ+2$ parton production and have found that the s -channel approximation overestimates the contribution of $qq \rightarrow qqZZ$ to a polarization measurement because of additional t -channel and non-resonant contributions. To be on the conservative side in our analysis, we include only the gluon fusion mechanism.

Higgs decay into two Z 's goes primarily into longitudinal Z 's. It is this effect which we exploit in our analysis of the signal. The large irreducible background to $pp \rightarrow H \rightarrow ZZ$ is continuum production of Z pairs via $q\bar{q} \rightarrow ZZ$. The dominant contribution to this background rate comes from production of a pair of transverse Z 's.

The main reducible background is from QCD corrections to single Z production: a Z is produced at large transverse momentum, which decays into an $\ell^+\ell^-$ pair, and is accompanied by jets that are missed in the detector because they go down the beam pipe. To model this background, we use the matrix elements for $q\bar{q} \rightarrow Zg \rightarrow e^+e^-g$ and crossed diagrams. We count in the background rate only the part of the cross section where the charged leptons have rapidity $|y_\ell| < y_\ell^c$, so that they are in the central region, and a large final state parton rapidity $|y_p| > y_p^c$.

In Fig. 1, we show the transverse mass distribution for the three contributions above. Here, the transverse mass m_T is defined to be

$$m_T^2 = [(\vec{p}_T^2 + m_Z^2)^{1/2} + (\vec{p}_T^2 + m_Z^2)^{1/2}]^2 - (\vec{p}_T + \vec{p}_T)^2$$

where \vec{p}_T is the Z boson transverse momentum reconstructed from $\ell^+\ell^-$ momenta and \vec{p}_T is the missing transverse momentum. In our Monte Carlo, with these three processes, all contributions have balanced p_T : $\vec{p}_T = -\vec{p}_T$. The dashed line in the figure indicates the gluon fusion production of a 500 GeV Higgs, the solid line shows the continuum production of ZZ and the dot-dashed line shows the rate from QCD production of Z +missing jet. Here the rapidity cuts of $y_p^c = y_\ell^c = 3$ are used, and in all the figures, a charged lepton transverse momentum cut of $p_T > 20$ GeV is applied. The heavy solid line is the total of the three contributions.

A longitudinal polarization vector for a massive particle, subjected to an arbitrary boost, will not, in general, retain its longitudinal character, so the statement that the $Z_L Z_L$ production rate is enhanced by a specific amount in Higgs production is a frame dependent statement. For a sufficiently heavy Higgs, the parton center of mass frame

(the Higgs rest frame) and the hadron center of mass frame coincide.

Fig. 1. The transverse mass distributions for $gg \rightarrow H \rightarrow ZZ \rightarrow \ell^+ \ell^- \nu \bar{\nu}$ (dashed), $q\bar{q} \rightarrow ZZ \rightarrow \ell^+ \ell^- \nu \bar{\nu}$ (solid) and $q\bar{q} \rightarrow Zg \rightarrow \ell^+ \ell^- g$, with crossed diagrams, (dot-dashed) for pp collisions at $\sqrt{S} = 14$ TeV. Here, the lepton rapidity is $|y_\ell| < 3$ and the final state parton rapidity is $|y_p| > 3$ to mimic a missing jet.

The decay distributions of the lepton from Z_L and Z_T decays, in the Z rest frame, are

$$\phi_L(z) = \frac{3}{4}(1 - z^2) \quad \phi_T(z) = \frac{3}{8}(1 + z^2) \quad (1)$$

where $z = \cos\theta$ for θ , the angle between the lepton and the axis defined by the Z momentum in the parton center of mass frame. The shape of the decay distribution as well as the average value of $|z|$ (for longitudinally polarized Z 's, a value of $3/8$, and for transversely polarized Z 's, a value of $9/16$) characterize the production mechanism. These decay distributions for the gold plated modes have been discussed elsewhere.⁵ For the Higgs decay into ZZ where one Z decays into neutrinos, one loses the information required to reconstruct the parton center of mass.

Note that in the parton center of mass frame (pcm), $z = -2\vec{p}_\ell^{pcm} \cdot \vec{\epsilon}_L^{pcm}/M_Z$, where we have a four-vector dot product which involves the longitudinal polarization vector $\vec{\epsilon}_L^{pcm}$. The parton center of mass frame differs from the hadron center of mass frame by a boost, however, the Lorentz boost of $\vec{\epsilon}_L^{pcm}$ converts the four vector into a linear combination of longitudinal and transverse polarization vectors. If the Higgs is heavy enough, the boost will not be large. To approximate $|z|$ in the hadron center of mass, we introduce the variable z^* where $z^* = 2|\vec{p}_\ell \cdot \vec{\epsilon}_L|/M_Z$. Here, all of the vectors are in the hadron center of mass, and $\vec{\epsilon}_L = (|\vec{p}_Z|/M_Z, E_z \vec{p}_Z/(|\vec{p}_Z| M_Z))$ is the longitudinal polarization vector determined from the reconstructed Z momentum. In the results presented below, we plot the average value of z^* as a function of transverse mass.

3. Results

We now show our results for several values of the Higgs mass. In Fig. 2, we show $\langle z^* \rangle$ as a function of m_T for $m_H = 600$ GeV, where the input top quark mass is taken at $m_t = 175$ GeV. The triangles show the $\langle z^* \rangle$ value for the combination of ZZ continuum production and the QCD missing jet background, and the squares are for the gluon fusion Higgs signal. For each of the separate cross sections σ_i , $i = c$

(continuum), m (missing jet background) and h (Higgs signal), the overall $\langle z^* \rangle$ value is determined by

$$\langle z^* \rangle = \frac{\langle z^* \rangle_h \sigma_h + \kappa(\langle z^* \rangle_m \sigma_m + \langle z^* \rangle_c \sigma_c)}{\sigma_h + \kappa(\sigma_m + \sigma_c)} \quad (2)$$

with $\kappa = 1$. In order to estimate the error on the theoretical prediction for $\langle z^* \rangle$, we also take $\kappa = 1 \pm 0.3$. This error from the normalization uncertainty from non-Higgs cross sections is combined in quadrature with a statistical error. The statistical error is estimated by $\langle z^* \rangle / \sqrt{N_{evt}}$, where the number of events assumes an integrated luminosity of 10^5 pb^{-1} . The combined error is the outer error bar, with only the statistical error indicated by the inner vertical error bar on the figures. We take a transverse mass bin width of 50 GeV, except for the two last bins, where the widths are 100 GeV and 250 GeV, respectively, to include a reasonable number of events. The statistical error dominates the overall error. This figure and Figs. 3a and 3b below use $y_\ell^c = y_p^c = 3.0$. Figure 3a shows $\langle z^* \rangle$ versus m_T for $m_H = 400 \text{ GeV}$, while Fig. 3b has $m_H = 800 \text{ GeV}$. In all of these figures, only one charged lepton family is included in the rate.

Fig. 2. The value of $\langle z^* \rangle$ as a function of m_T for $m_H = 600 \text{ GeV}$ and $m_t = 175 \text{ GeV}$. Rapidity cuts applied are $y_\ell^c = y_p^c = 3.0$. The symbols are described in the text.

At the LHC, a more realistic set of rapidity cuts is to include charged leptons in a more central region, with $y_\ell^c = 2.5$, and to put the “missing jet” cut at $y_p^c = 4$ for the parton rapidity. With these cuts, the signal event rate is not reduced very much, but the QCD missing jet background is greatly reduced. Figures 4a and 4b show $\langle z^* \rangle$ versus m_T for $m_H = 400 \text{ GeV}$ and $m_H = 800 \text{ GeV}$, respectively, with these new rapidity cuts. Again, the error bars indicate the combined normalization and statistical error bars as described above.

Figures 2-4 indicate that the value of $\langle z^* \rangle$ will be a useful tool to characterize high transverse mass data at the LHC. With an integrated luminosity of 10^5 pb^{-1} ,

Higgs masses up to 800 GeV are accessible using this method.

Fig. 3. Value of $\langle z^* \rangle$ for m_T bins with a) $m_H = 400$ GeV and b) $m_H = 800$ GeV, with $y_\ell^c = y_p^c = 3$.

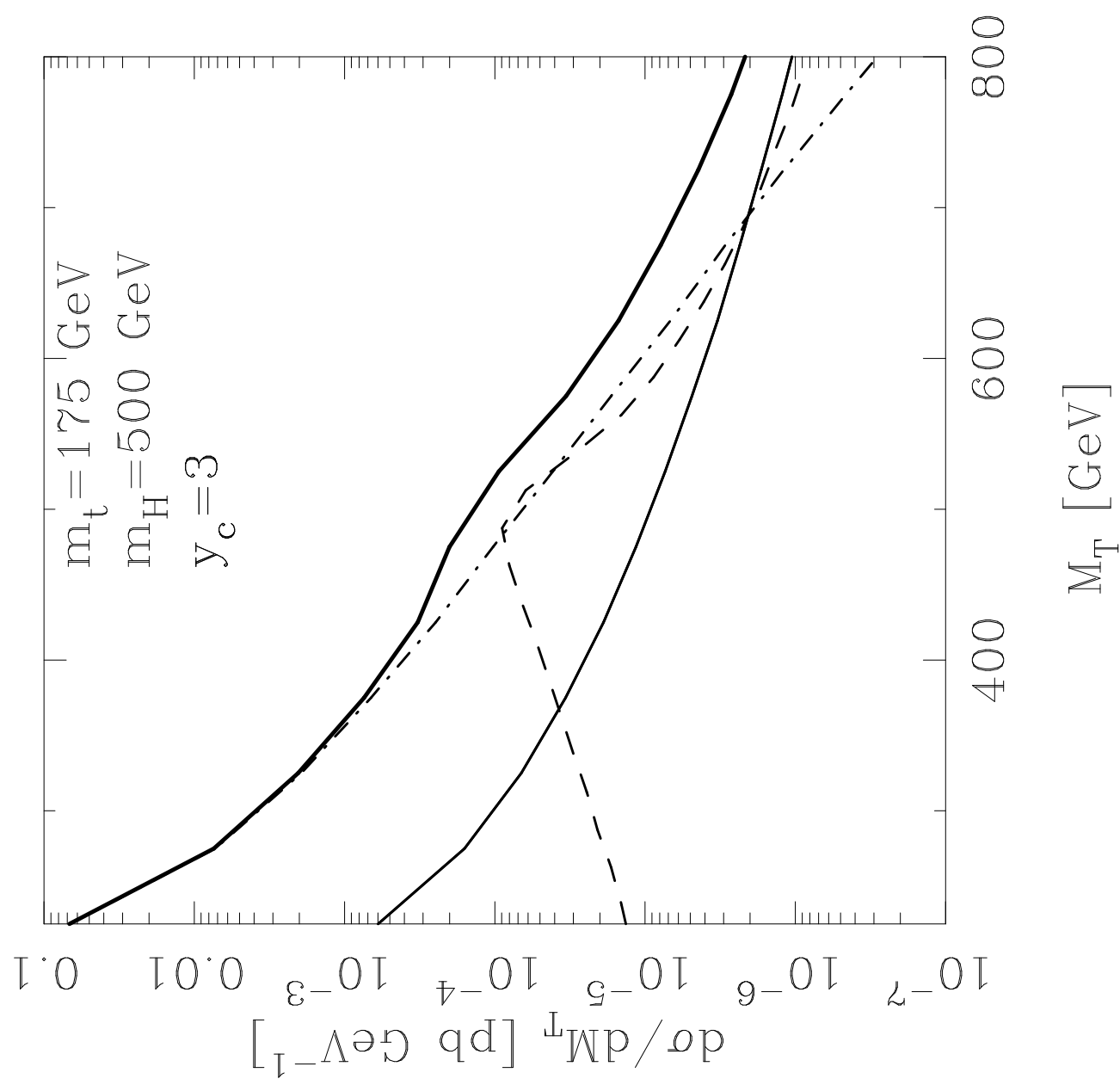
Fig. 4. As in Fig. 3, but with $y_\ell^c = 2.5$ and $y_p^c = 4$.

References

1. R. N. Cahn, *et al.*, in *Experiments, Detectors and Experimental Areas for the SSC*, proceedings of the Workshop, Berkeley, CA, 1987, eds. R. Donaldson and M. Gilchriese (World Scientific, Singapore, 1988).
2. B. W. Lee, C. Quigg and H. B. Thacker, *Phys. Rev. Lett.* **38** (1977) 883; *Phys. Rev.* **D16** (1977) 1519.
3. R. N. Cahn and M. S. Chanowitz, *Phys. Rev. Lett.* **56** (1986) 1327.
4. V. Barger, T. Han and R. J. N. Phillips, *Phys. Rev.* **D36** (1987) 295.
5. M. J. Duncan, *Phys. Lett.* **B179** (1986) 393; T. Matsuura and J. J. van der Bij, *Z. Phys.* **C51** (1991) 259.
6. M. J. Duncan, G. L. Kane and W. W. Repko, *Nucl. Phys.* **B272** (1986) 517; G. L. Kane and C. P. Yuan, *Phys. Rev.* **D40** (1989) 2231.
7. M. J. Duncan and M. H. Reno, in *Proceedings of the Workshop on Physics at Current Accelerators and Supercolliders*, Argonne National Laboratory, 1993, eds. J. L. Hewett, A. R. White and D. Zeppenfeld.
8. J. F. Gunion, H. E. Haber, F. E. Paige, Wu-Ki Tung and S. S. D. Willenbrock, *Nucl. Phys.* **B294** (1987) 621.
9. U. Baur and E. W. N. Glover, *Nucl. Phys.* **B347** (1990) 12.

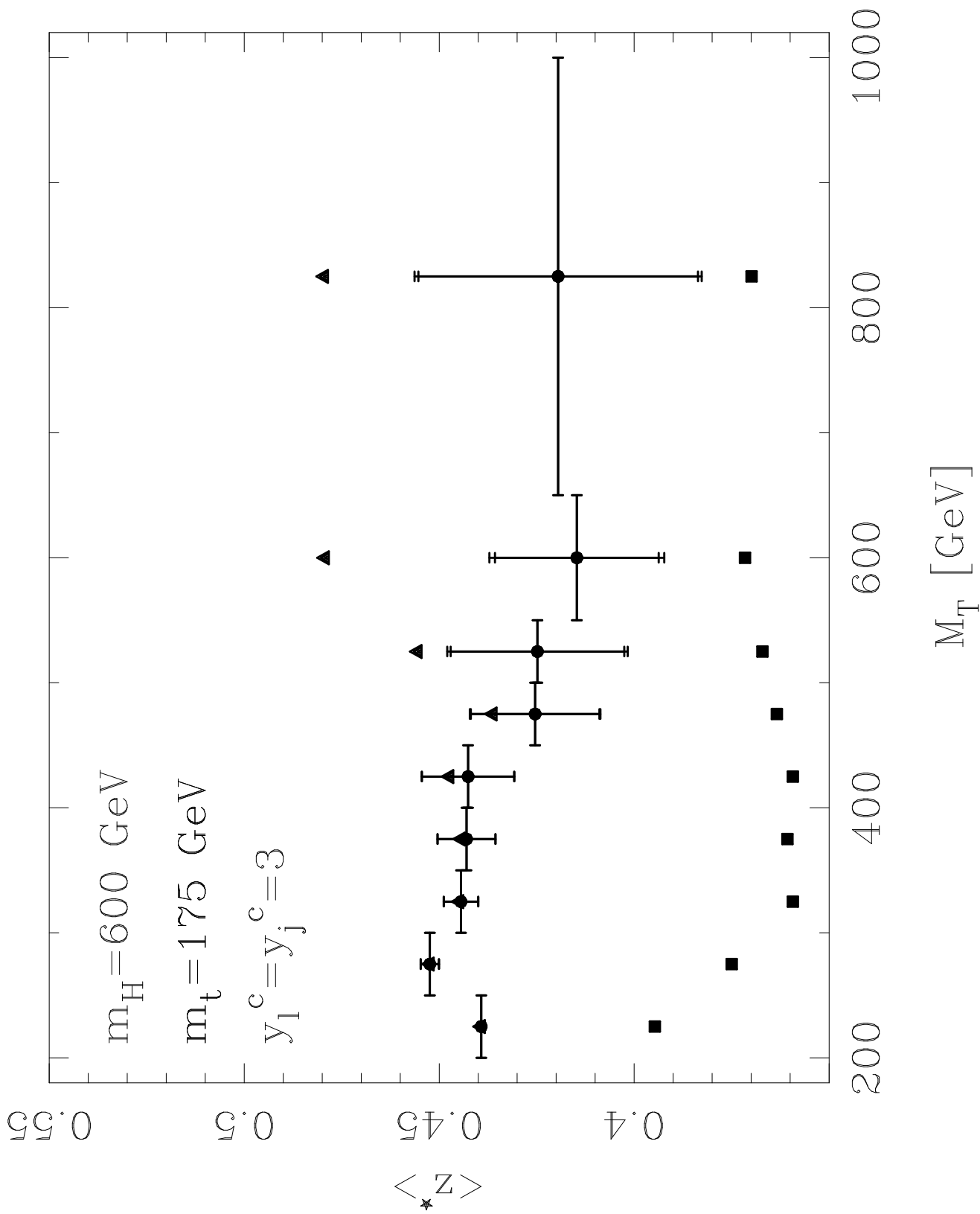
This figure "fig1-1.png" is available in "png" format from:

<http://arxiv.org/ps/hep-ph/9409334v1>



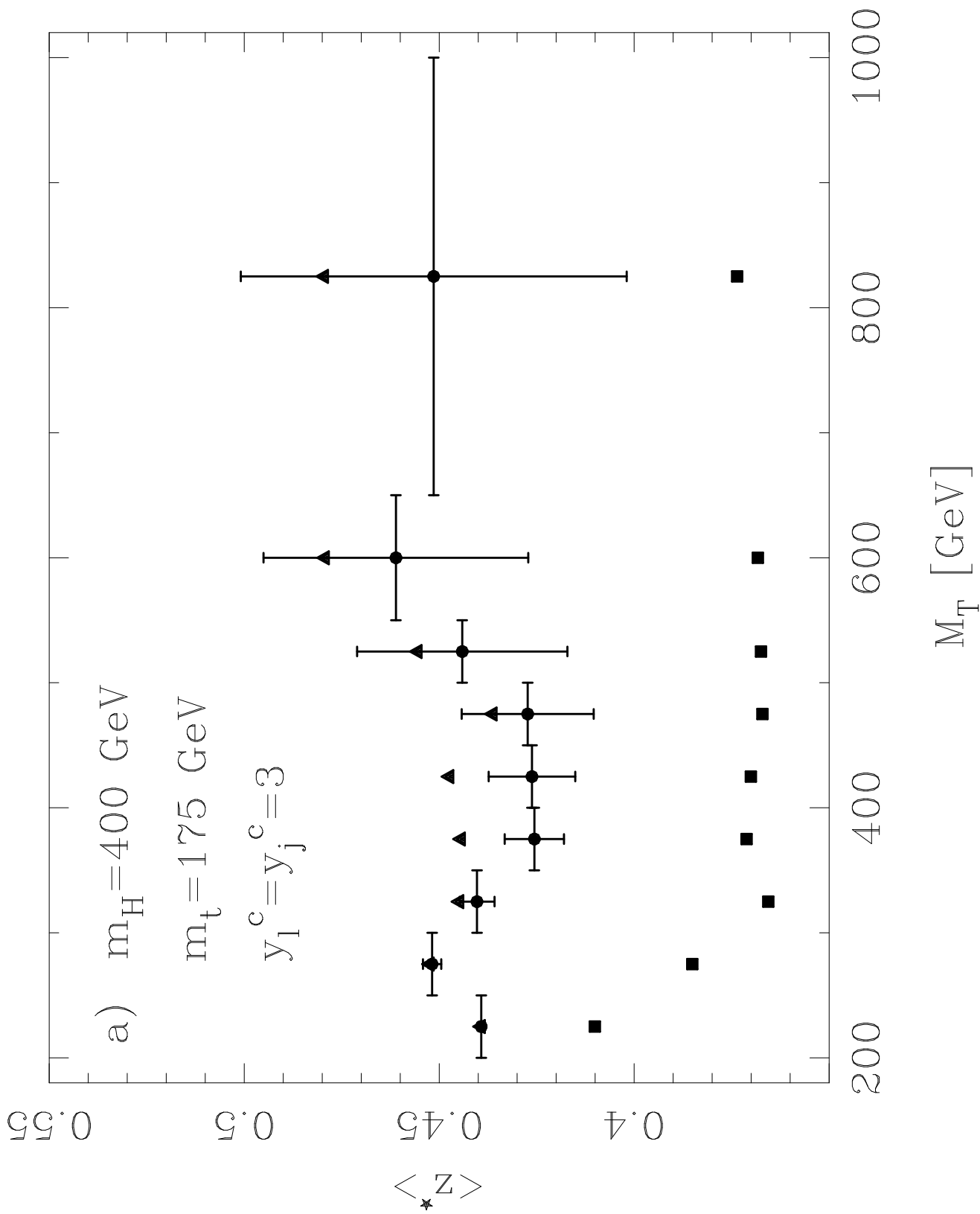
This figure "fig1-2.png" is available in "png" format from:

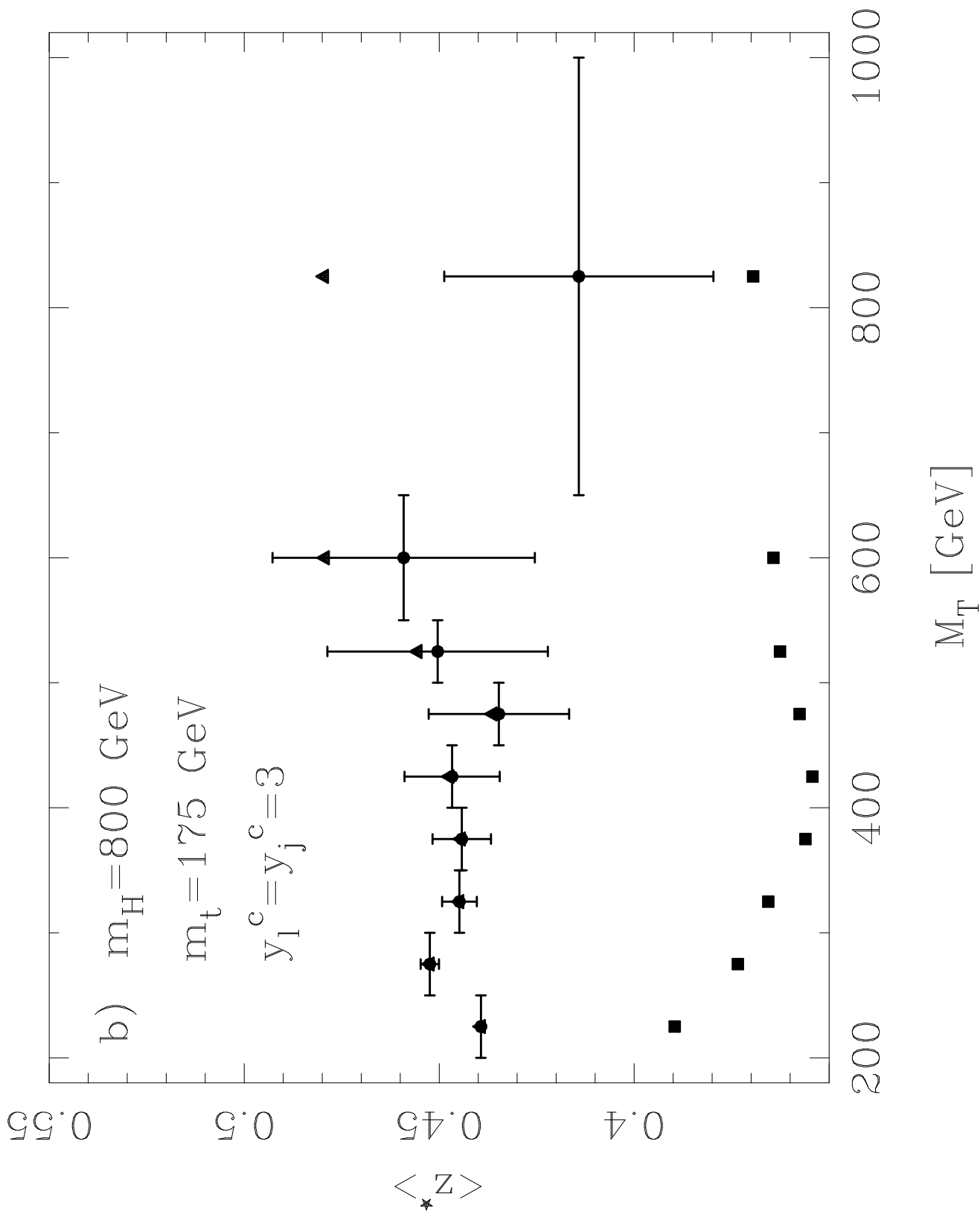
<http://arxiv.org/ps/hep-ph/9409334v1>



This figure "fig1-3.png" is available in "png" format from:

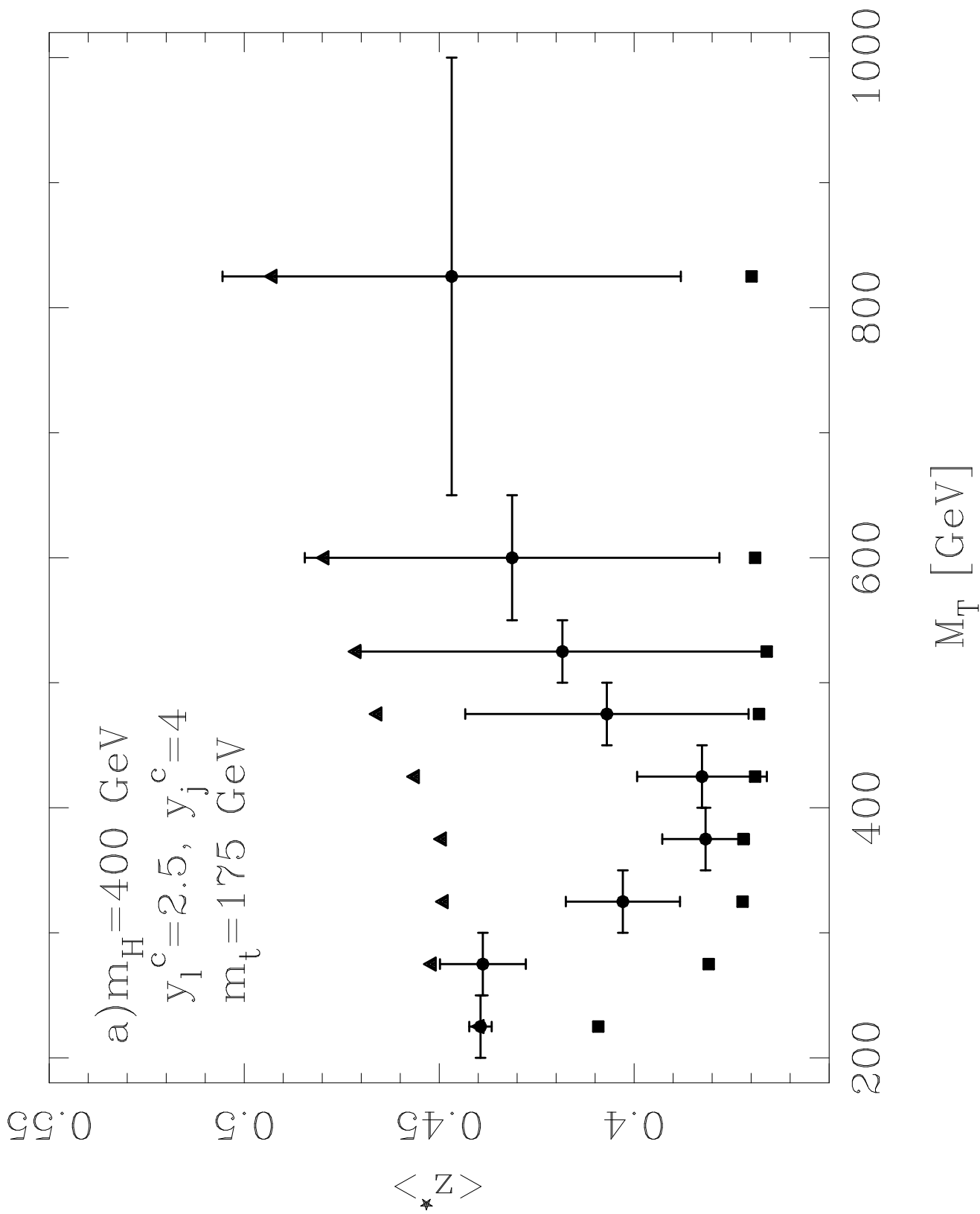
<http://arxiv.org/ps/hep-ph/9409334v1>

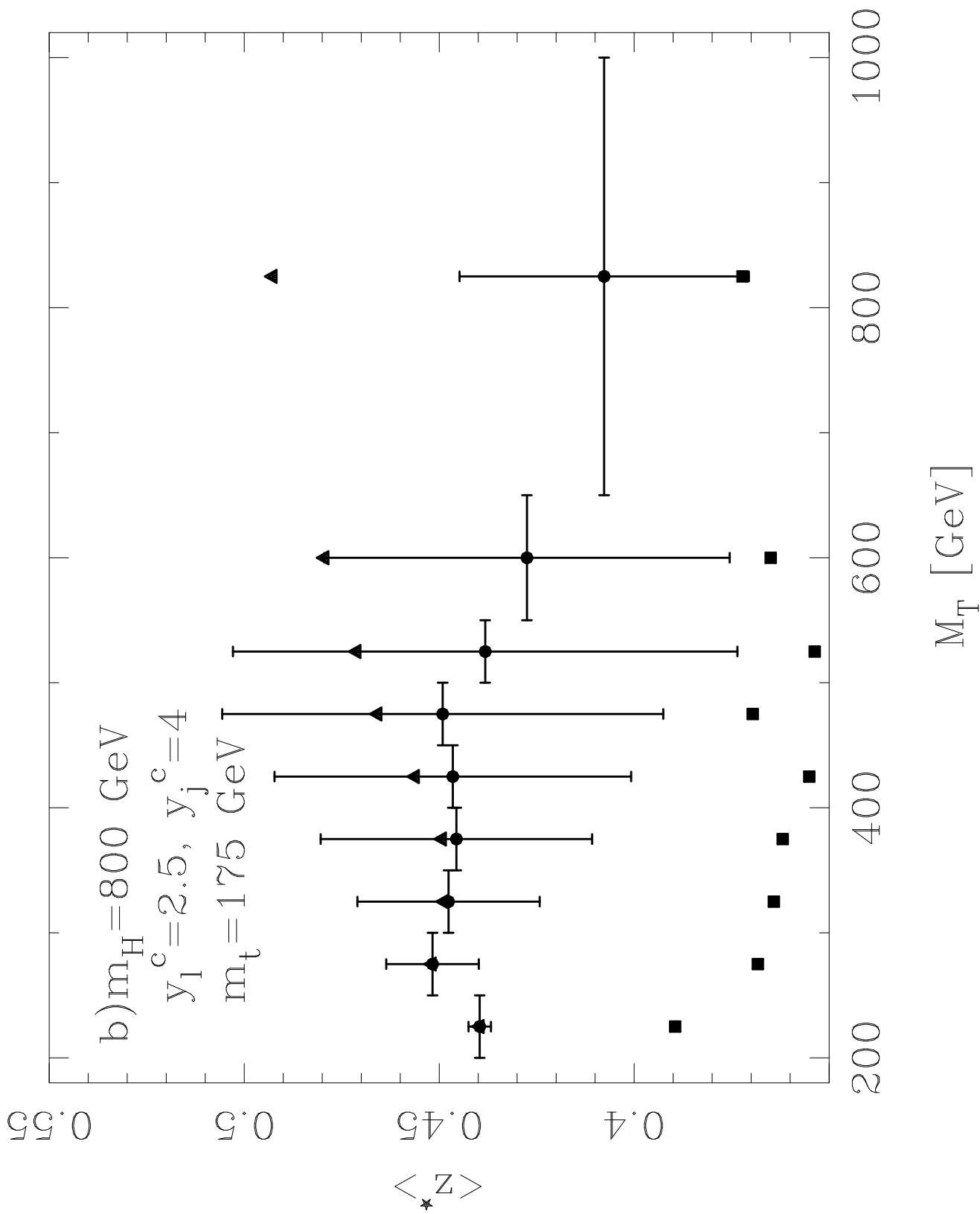




This figure "fig1-4.png" is available in "png" format from:

<http://arxiv.org/ps/hep-ph/9409334v1>





This figure "fig1-5.png" is available in "png" format from:

<http://arxiv.org/ps/hep-ph/9409334v1>

This figure "fig1-6.png" is available in "png" format from:

<http://arxiv.org/ps/hep-ph/9409334v1>